

Discovery, SAR, and Pharmacokinetics of a Novel 3-Hydroxyquinolin-2(1H)-one Series of Potent D-Amino Acid Oxidase (DAAO) Inhibitors[†]

Allen J. Duplantier,* Stacey L. Becker, Michael J. Bohanon, Kris A. Borzilleri, Boris A. Chrnyk, James T. Downs, Lain-Yen Hu, Ayman El-Kattan, Larry C. James, Shenping Liu, Jiemin Lu, Noha Maklad, Mahmoud N. Mansour, Scot Mente, Mary A. Piotrowski, Subas M. Sakya, Susan Sheehan, Stefanus J. Steyn, Christine A. Strick, Victoria A. Williams,[‡] and Lei Zhang

Pfizer Global Research and Development, Groton Laboratories, Eastern Point Road, Groton, Connecticut 06340

Received February 2, 2009

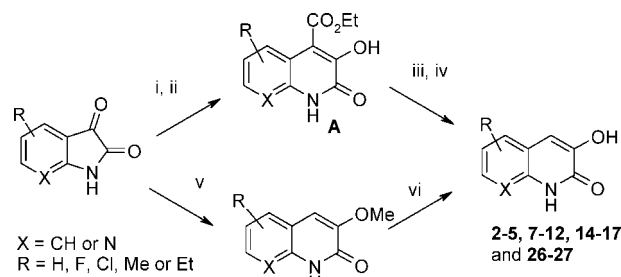
3-Hydroxyquinolin-2(1H)-one (**2**) was discovered by high throughput screening in a functional assay to be a potent inhibitor of human DAAO, and its binding affinity was confirmed in a Biacore assay. Cocrystallization of **2** with the human DAAO enzyme defined the binding site and guided the design of new analogues. The SAR, pharmacokinetics, brain exposure, and effects on cerebellum D-serine are described. Subsequent evaluation against the rat DAAO enzyme revealed a divergent SAR versus the human enzyme and may explain the high exposures of drug necessary to achieve significant changes in rat or mouse cerebellum D-serine.

Introduction

D-Serine, a coagonist at the glycine site on the *N*-methyl D-aspartate (NMDA) receptor,¹ is synthesized from L-serine by serine racemase and is metabolized by D-amino acid oxidase (DAAO^a). Because phencyclidine (PCP), a noncompetitive antagonist of the NMDA receptor, has been shown to produce effects in healthy volunteers resembling the positive, negative, and cognitive symptoms of schizophrenia,² it has been proposed that increasing function of this receptor, perhaps by inhibiting the breakdown of D-serine by DAAO, may ameliorate schizophrenic symptoms.³ In support of this idea, several factors have linked low levels of D-serine to schizophrenia: (1) D-serine levels in serum and CSF have been reported to be decreased in schizophrenia patients vs healthy controls,^{4,5} (2) in schizophrenia patients, DAAO activity and expression have been reported to be increased,^{6–8} and (3) in small controlled clinical studies, oral administration of D-serine (30 mg/kg/day) improved positive, negative, and cognitive symptoms of schizophrenia as add-on therapy to typical and atypical antipsychotics,^{9,10} with the exception of clozapine.¹¹ It has been suggested that coadministration of D-serine with a DAAO inhibitor may be a more effective means of delivering D-serine to the brain.¹²

Reported DAAO inhibitors such as benzoic acid,¹³ 5-methylpyrazole-3-carboxylic acid (AS057278),¹⁴ 6-chlorobenzo-*[d]*-isoxazol-3-ol (CBIO),¹² and 5-carboxyfuro[3,2-*b*]pyrrole (**1**)¹⁵ are small aryl carboxylic acids or acid-isosteres that are ionized (pK_a 's = 4–5) at the peroxisomal pH of ~8.2. High-throughput screening of our compound file against the human DAAO enzyme uncovered lead compounds with pK_a 's > 8 that are not completely ionized within the peroxisome. Herein, we report the binding mode, SAR, and pharmacokinetics of 3-hydroxyquinolin-2(1H)-one (**2**, pK_a = 8.7) and its analogues as potent and novel DAAO inhibitors (Chart 1).

Scheme 1^a



^a Reagents and conditions: (i) ethyl diazoacetate, diethylamine, EtOH, RT, 2 d; (ii) 1 N HCl, RT, 12 h; (iii) LiOH (10 equiv), 1:1 MeOH/water, 150 °C, microwave, 2 h; (iv) 1 N HCl, RT; (v) (TMS)diazomethane, diethylamine, EtOH, RT, 18 h; (vi) BBr₃ (3 equiv), CH₂Cl₂, -78 °C to RT, 3 h.

Chemistry. The construction of the quinolinone ring has recently been reviewed,¹⁶ and several syntheses of compound **2** have been reported in the literature: (a) ring expansion reaction of isatin with diazomethane,¹⁷ (b) Eistert ring expansion of isatin with ethyl diazoacetate,¹⁸ and (c) treatment of 2-aminobenzaldehyde with chloroacetic anhydride.¹⁹ In addition, syntheses of some chloro (**7**,¹⁷ **8**,²⁰ and **9**¹⁹), methyl (**13**,¹⁹ **23**,²¹ **24**,²² and **25**²³) and pyridyl (**18**²⁴) analogues of **2** have also been reported (see Table 1 for structures). Modified versions of the literature routes for **2** starting from the appropriate isatin were used for the preparation of compounds **2–5**, **7–12**, **14–17**, and **26–27** (Scheme 1). Intermediate “A” (Scheme 1) was obtained in 40–85% yields by treatment of the appropriate isatin with ethyl diazoacetate in the presence of diethylamine over a couple of days followed by addition of dilute aqueous HCl. The resulting ethyl ester was saponified and decarboxylated in the microwave at 150 °C over two hours to provide 6-, 7-, and 8- substituted 3-hydroxyquinolin-2(1H)-ones in low (<20%) to moderate (>50%) yields. 5-Substituted analogues did not decarboxylate under these conditions. Alternatively, substituted isatins were treated with TMS-diazomethane in the presence of diethylamine to provide methoxy intermediates “B” (Scheme 1), which were then demethylated with boron tribromide.²⁵ The 7-azaisatin reagent needed for the synthesis of **27** (compound

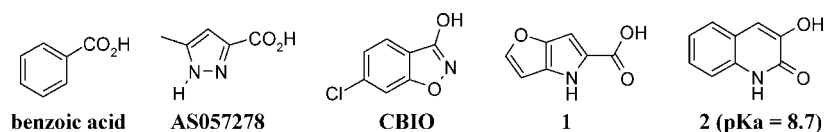
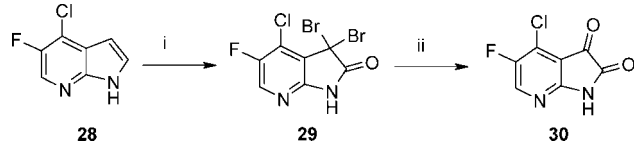
[†] Protein Data Bank: PDB ID number 3G3E.

* To whom correspondence should be addressed. Phone: 860-441-6009. Fax: 860-715-2350. E-mail: allen.j.duplantier@pfizer.com.

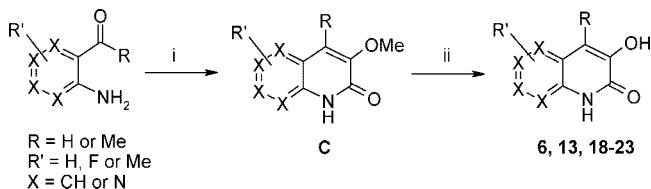
[‡] Current address: Westhill High School, Stamford, CT.

^a Abbreviations: DAAO, D-amino acid oxidase; DDO, D-aspartate oxidase; FAD, flavin adenine dinucleotide; HRP, horseradish peroxidase; NMDA, *N*-methyl D-aspartate; CSF, cerebral spinal fluid; SAR, structure–activity relationship.

Chart 1

Scheme 2^a

^a Reagents and conditions: (i) NBS (4 equiv), *tert*-BuOH, RT, 2 h, 97%; (ii) silver trifluoroacetate (2 equiv), 5% water/CH₃CN, darkness, 3 h, 5%.

Scheme 3^a

^a Reagents and conditions: (i) ethyl methoxyacetate (3 equiv), lithium bis(trimethylsilyl)amide (3 equiv), THF, -78 °C, 20 min, then amino aldehyde, -78 °C to RT over 18 h, then 6 N HCl, reflux, 2 h; (ii) BBr₃ (3 equiv), CH₂Cl₂, -78 °C to RT, 3 h.

30) was prepared from azaindole **28** by reaction with NBS followed by silver trifluoroacetate (Scheme 2).²⁶ In cases where an isatin starting material was not readily available, the corresponding aryl amino aldehyde (or ketone) was condensed with the enolate of ethyl methoxyacetate to provide methoxy intermediate "C" (Scheme 3), which was subsequently demethylated with boron tribromide (compounds **6**, **13**, and **18–23**).

Biology. Potencies of compounds were determined in a cell free fluorescence assay using recombinant human or rat DAAO in which the H₂O₂ generated from the degradation of D-serine was linked to oxidation of Amplex Red in the presence of horseradish peroxidase (HRP). A comparable assay using recombinant human D-aspartate oxidase (DDO) was run to determine selectivity against DDO,²⁷ the closest human homologue to DAAO, and to eliminate any artifact arising from inhibition of HRP. Binding affinity and kinetics were measured using biotinylated recombinant human DAAO bound to a Neutravidin surface in a Biacore binding assay. In vivo activity of selected compounds was established by LC/MS-MS quantitation of D-serine in cerebellum extracts from male Sprague–Dawley rats or male 129 SVEV mice treated with inhibitors.

Structure Based Drug Design. Compound **2** was cocrystallized with the *h*-DAAO enzyme. The X-ray structure of **2** bound to *h*-DAAO (Figure 1) shows the 3-hydroxyl group involved in two hydrogen bonds, one with the Tyr228–OH and the other with the Arg283–NH. Additional interactions to the Arg residue are made by the 2-carbonyl group of **2**, while the lactam –NH donates a hydrogen bond to the backbone carbonyl of Gly313. Consistent with similar structures of aryl acids bound to DAAO,²⁸ compound **2** forms a π – π stacking interaction with the *re*-face of the flavin ring of flavin adenine dinucleotide (FAD). The aryl chain of Tyr224 stacks on the other side of compound **2**. Because all reported DAAO inhibitors^{12–15} have an aromatic moiety that is likely involved in similar π – π stacking interactions with FAD and Tyr224, these interactions are considered important to compound **2** binding and are

reserved in subsequently designed compounds. Figure 2 is a schematic diagram comparing the bonding interactions of compound **2** with those of benzoic acid. As seen in Figures 1 and 2, the aryl ring of **2** is in contact with multiple hydrophobic residues (Ile230, Leu215, Leu51, and Gln63), leaving no room for large multiatom substitution off of that ring.

Structure optimization studies were initially based on the predicted binding interactions of compound **2** with the enzyme active site. Compound **2** was docked into a cocrystallized *h*-DAAO–benzoic acid structure²⁹ using our in-house AG-DOCK-docking program.³⁰ It was observed that 3-hydroxyquinolin-2(1H)-ones dock to DAAO in the same manner as do small carboxylic acid inhibitors. All interactions observed from the X-ray structure of **2** are conserved in the AGDOCK conformation of **2** and its close-in analogues. Perhaps due to the simplicity of the binding site and the directionality afforded by the polar interactions, docking of **2** and benzoic acid appear largely straightforward, with the top ranked pose nearly identical to the observed X-ray structure. In addition, the docking score³¹ shows a reasonable correlation ($R^2 = 0.43$) to the observed binding activity for the ligands reported in Table 1 and is better correlated to the observed activity than either simple physical property descriptors (molecular weight, calculated log P, or polar surface area) or orbital parameters (electronegativity, orbital hardness).

Using the docking score as a tool to help define which substituents would best fit in the binding pocket pointed clearly to smaller substituents as being most favorable. Figure 3 shows a box-plot representation of possible monosubstituted analogues of compound **2** ordered by heavy atom count along the *x*-axis. Here, 12 heavy atoms refers to the parent compound (**2**) as well as 4 possible 3-hydroxy-naphthyridin-2(1H)-one analogues (compounds **18–21**); 13 heavy atoms refers to methyl, fluoro and chloro (compounds **3–14**); 14 heavy atoms refers to ethyl, cyano, and methoxy (compounds **15–17**); 15 atoms refers to *n*-propyl and *iso*-propyl, and 18 heavy atoms refers to phenyl substituted compounds. Compounds with 12 and 13 heavy atoms scored the best, with an average predicted IC₅₀ below 10 nM, while compounds with 14 heavy atoms were predicted to be much less active (~50 nM). *iso*-Propyl and *n*-propyl substituents were all predicted to have significantly diminished potency and were not synthesized. The phenyl substituted compounds simply can not fit in the active site, and the resulting unreliable docking scores reflect impossible thermodynamic interactions of overlapping bonds. This analysis reinforced the prediction that larger substitutions would be detrimental to activity and, in addition, only monofluoro substitutions were predicted to improve potency beyond that of compound **2**.

Results and Discussion

Compound **2** was reported in the literature to be a weak inhibitor of [³H]-glycine binding to the site associated with the NMDA receptor (29% inhibition at 10 μ M)¹⁷. In our hands, **2** was found to be a potent inhibitor of *h*-DAAO (IC₅₀ = 4 nM) with good selectivity against *h*-DDO (IC₅₀ = 855 nM). Parallel evaluation of **2** for stability in human microsomes suggested low metabolic clearance, and a low MDR/MDCK ratio³² (0.35)

Table 1. Human and Rat in Vitro Potencies of Compounds 1–27

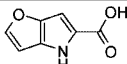
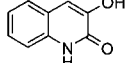
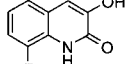
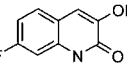
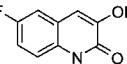
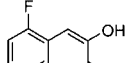
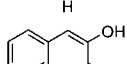
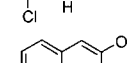
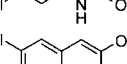
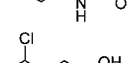
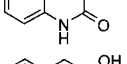
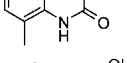
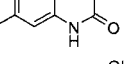
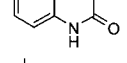
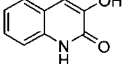
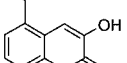
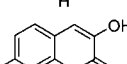
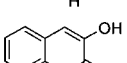
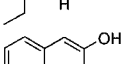
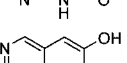
Compd	Structure	<i>h</i> -DAAO IC ₅₀ , nM () ^a	<i>h</i> -DDO IC ₅₀ nM ^b	<i>r</i> -DAAO IC ₅₀ nM ^c
1		9 (7-13, n = 10)	>19,500 (n = 3)	424 ± 112 (n = 7)
2		4 (3-5, n = 76)	855 (n = 32)	215 ± 55 (n = 5)
3		3 (2-7, n = 8)	4,620 (n = 5)	180 ± 28 (n = 3)
4		10 (7-16, n = 8)	22,400 (n = 3)	1,445 ± 145 (n = 2)
5		9 (4-22, n = 9)	>8,880 (n = 6)	308 ± 58 (n = 2)
6		8 (4-16, n = 8)	64,000 (n = 1)	196 ± 25 (n = 2)
7		33 (22-49, n = 8)	>43,400 (n = 4)	8,720 ± 1240 (n = 2)
8		100 (51-196, n = 4)	>50,000 (n = 2)	ND
9		155 (66-361, n = 4)	>50,000 (n = 2)	ND
10		4 (2-6, n = 10)	206,000 (n = 1)	40 ± 3 (n = 2)
11		38 (18-78, n = 4)	31,600 (n = 1)	ND
12		197 (158-245, n = 6)	21,500 (n = 3)	ND
13		2,750 (n = 1)	ND	ND
14		16 (6-47, n = 8)	54,600 (n = 3)	8,470 ± 1050 (n = 2)
15		8 (7-9, n = 4)	61,900 (n = 1)	3,665 ± 265 (n = 2)
16		22,600 (n = 1)	ND	ND
17		14,400 (4800-34500, n = 2)	>50,000 (n = 1)	ND
18		8 (6-11, n = 7)	>7,640 (n = 4)	200 ± 15 (n = 2)
19		32 (26-40, n = 9)	>36,000 (n = 5)	3,081 ± 395 (n = 2)
20		784 (582-1060, n = 7)	>50,000 (n = 3)	ND

Table 1. Continued

Compd	Structure	<i>h</i> -DAAO IC ₅₀ , nM () ^a	<i>h</i> -DDO IC ₅₀ nM ^b	<i>r</i> -DAAO IC ₅₀ nM ^c
21		128 (45-365, n = 4)	>50,000 (n = 2)	ND
22		>50,000 (n = 4)	>50,000 (n = 2)	ND
23		17,300 (13700-21700, n = 4)	32,300 (n = 2)	ND
24		>26,200 (n = 4)	ND	ND
25		3,260 (n = 1)	ND	ND
26		5 (2-11, n = 8)	>43,200 (n = 4)	50 ± 13 (n = 2)
27		3 (2-4, n = 6)	>14,500 (n = 4)	4 ± 1 (n = 2)

^a Human D-amino acid oxidase assay, geometric mean (95% confidence interval). ^b Human D-aspartate oxidase assay. ^c Rat D-amino acid oxidase assay, mean ± SD.

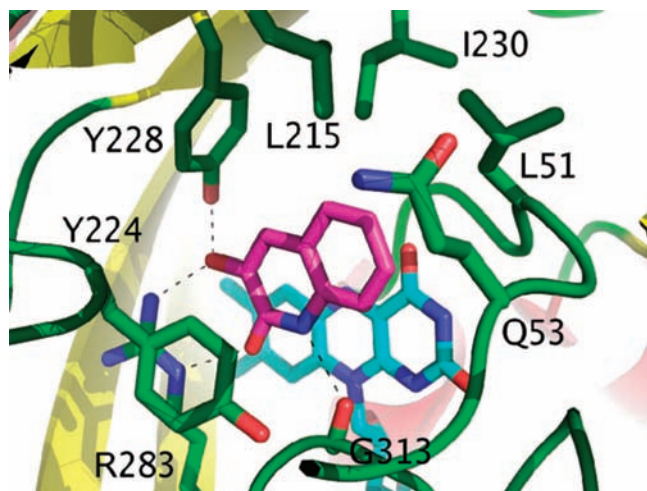


Figure 1. Compound **2** (carbon atoms in magenta and oxygen in red) at *h*-DAAO enzyme active site. Side chains of key interacting residues are shown with carbon colored in green and nitrogen in blue. Hydrogen bonding interactions are shown in dash. FAD is shown with carbons in cyan. The coordinates of this structure have been deposited in the Protein Data Bank (PDB ID number 3G3E).

for **2** meant that it was not likely a substrate for P-glycoprotein and thus should have a reasonable chance of getting across the blood–brain barrier (data not shown). In vivo PK studies of **2** in the rat revealed moderate clearance (46 mg/min/kg) and low oral bioavailability ($F = 0.9\%$), resulting in low oral plasma exposures ($C_{\max} = 5.5$ ng/mL) (see Table 2). To determine the ability of **2** to elevate cerebellum D-serine levels in the rat, we dosed **2** subcutaneously and found that a minimum effective dose of 56 mg/kg was required to significantly elevate D-serine by 2–4 fold above vehicle. At this dose, compound **2** was determined to have a brain/plasma ratio of 0.7 and a large

unbound fraction of drug in the brain ($F_{u\text{brain}} = 0.22$), and this translated into free brain exposures of 670 nM (160× over the *h*-DAAO IC₅₀ of 4 nM) at the 4 h time point. Because of solubility constraints in the vehicle, we were unable to increase the dose of **2** further. With the above data in hand, our goals for follow-up of **2** were to improve oral bioavailability and lower clearance while retaining nM potency and low molecular weight and ultimately to lower the dose of **2** required to see significant changes in D-serine levels.

Initial SAR development of the 3-hydroxyquinolin-2(1H)-one series was based on our understanding of the binding mode of **2** at the active site of the *h*-DAAO enzyme (Figures 1 and 2). Knowing that substitution of multi-atom groups around the aryl ring of **2** would not be allowed at the active site, we explored the effect of smaller groups by systematically substituting fluoro, chloro, methyl, and ethyl groups around the 5-, 6-, 7-, and 8-positions of the quinolinone ring (compounds **2**–**17**, Table 1). As the fluoro group was well tolerated in all positions (compounds **3**–**6**), compounds substituted with the larger chloro group displayed a range of *h*-DAAO activity with the 5-position (compound **10**) being most tolerated [IC₅₀ comparison: **2** = **10** (5-chloro) < **7** (8-chloro) < **8** (7-chloro) < **9** (6-chloro)]. The analogous methyl analogues followed a similar trend with the exception of the 6-methyl analogue **13** showing a more substantial decrease in *h*-DAAO activity (IC₅₀ = 2,750 nM). To test further the size limits of the *h*-DAAO active site, an ethyl group was evaluated at the 5-, 7-, and 8-positions. The 5-ethyl analogue (**15**) showed potent activity (IC₅₀ = 8 nM), but ethyl at the latter two positions (**16** and **17**) was detrimental to activity, thus confirming the small binding site. Substitution at the 4-position of the quinolinone ring was found to be unforgiving, as the 4-methyl analogue **23** was >4000× less active than **2**.

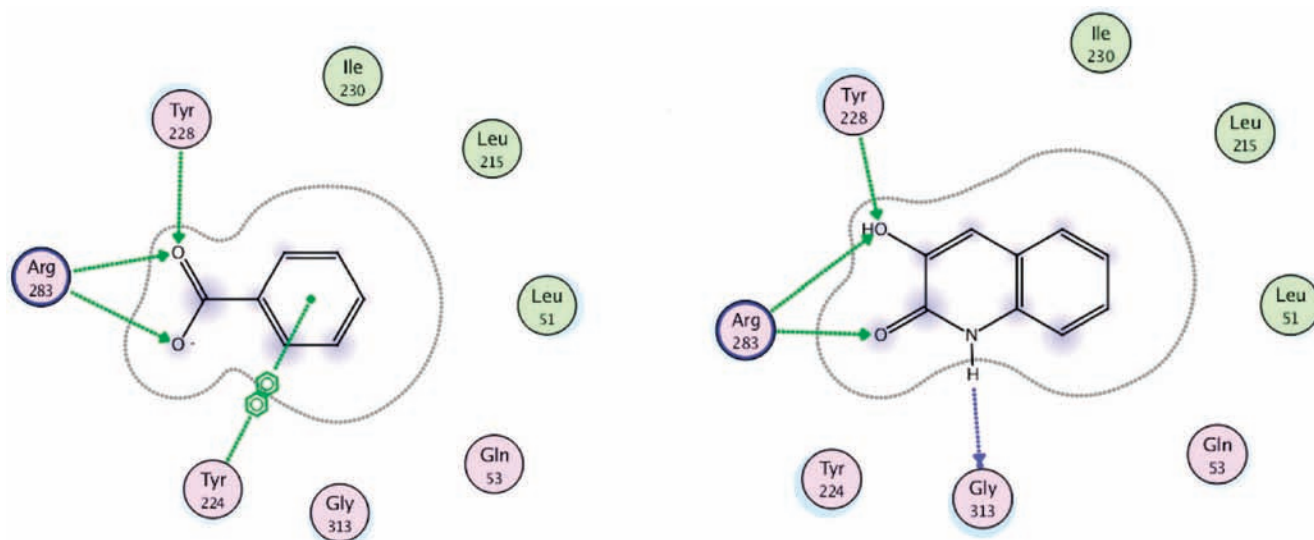


Figure 2. Schematic representation of residues in the (left) DAAO–benzoic acid X-ray structure, and (right) DAAO–compound **2** X-ray structure.

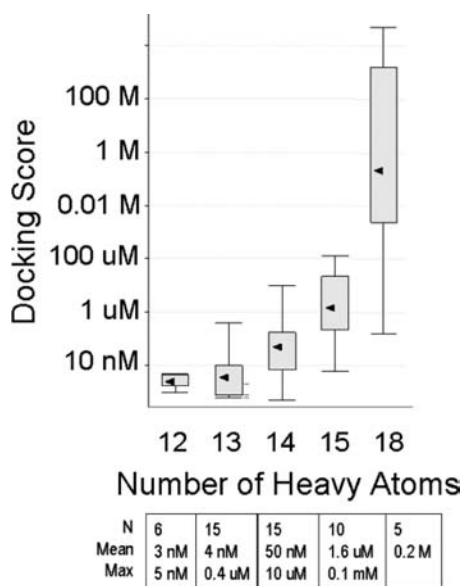


Figure 3. Analysis of Docking Score versus number of heavy atoms in analogues of **2**.

Table 2. Rat Pharmacokinetic Data (3 mg/kg, po; 1 mg/kg, iv)

comps	CLp (mL/min/kg)	V_d (L/kg)	$T_{1/2}$ (h)	%F	oral C_{max} (ng/mL)
2	46	10.8	ND	0.9	5.5
4	15	1.2	5.4	38	754
5	72	2.3	0.9	44	216

Disruption of the key hydrogen bond interaction of **2** with Arg283 (Figures 1 and 2) was accomplished by methylating the 3-hydroxy group (compound **24**). As predicted, **24** was rendered inactive without the H-bond interaction with Arg283. In a similar fashion, disrupting the interaction of **2** with Gly313 by methylating the amido nitrogen (compound **25**) also greatly reduced activity. These results led us to conclude that the amide and 3-hydroxy moieties of **2** were critical for nM potency.

In efforts to improve solubility, we prepared the four regiomeric naphthyridinone analogues of **2** (compounds **18–21**) as well as the pyridopyrazinone **22**. Of these heterocyclic analogues, **18** was the most active of the naphthyridinones ($IC_{50} = 8$ nM) and **22** was inactive. This latter result was surprising

Table 3. Human DAAO in Vitro Binding Data in Biacore Assay

comps	<i>h</i> -DAAO IC_{50} nM	<i>h</i> -DAAO K_D nM \pm SE	k_{on} ($M^{-1}s^{-1}$) \pm SE	k_{off} (s^{-1}) \pm SE
1	9	29 ± 2.3	$6 \pm 0.5 \times 10^4$	$2 \pm 0.05 \times 10^{-3}$
2	4	13 ± 0.5	$9 \pm 0.4 \times 10^4$	$1 \pm 0.02 \times 10^{-3}$
4	10	38 ± 0.9	$9 \pm 0.2 \times 10^4$	$4 \pm 0.02 \times 10^{-3}$
5	9	17 ± 2.7	$1 \pm 0.1 \times 10^5$	$2 \pm 0.2 \times 10^{-3}$
6	8	18 ± 3.2	$5 \pm 0.6 \times 10^4$	$8 \pm 1 \times 10^{-4}$
15	8	25 ± 0.6	$1 \pm 0.03 \times 10^5$	$3 \pm 0.03 \times 10^{-3}$
18	8	2 ± 0.2	$3 \pm 0.1 \times 10^5$	$6 \pm 0.6 \times 10^{-4}$

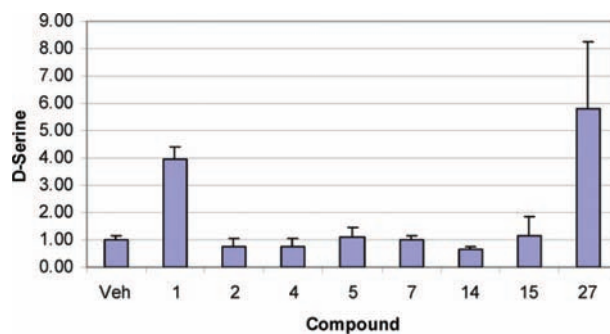


Figure 4. Cerebellum D-serine levels in mice (normalized to vehicle), 10 mg/kg, sc, 4 h post dose.

because independently replacing either of the two nitrogen atoms of **22** with carbon led to potent *h*-DAAO activity (compounds **18** and **21**).

To rule out that the aforementioned analogues of **2** were not inhibiting [3H]-glycine binding to the site associated with the NMDA receptor, compounds **2–6**, **10**, **14**, **15**, and **18** were evaluated³³ and all were found to have <50% inhibition at 10 μ M (data not shown). Therefore, we were not concerned that this class of DAAO inhibitors would compete with D-serine at the NMDA receptor.

Selected compounds from Table 1 were screened in rats for plasma exposures after oral administration at 3 mg/kg (data not shown). Of the compounds screened, the 7- and 6-fluoroquinolinones (**4** and **5**) displayed the highest C_{max} (754 and 216 ng/mL, respectively), and further PK studies revealed good oral bioavailability for both (see Table 2). In addition, **4** was shown to have low clearance and a reasonable half-life ($T_{1/2} = 5.4$ h).

Table 4. Mouse Exposure Data (10 mg/kg, sc, 4 h)

comps	[plasma] (nM)	Fu (plasma)	[plasma] _{free} (nM)	[brain] (nM)	Fu (brain)	[brain] _{free} (nM)	B/P
1	1340	0.95	1270	1120	1.0	1120	0.8
2	28	0.43	12	56	0.26	15	2.0
27	1620	0.11	178	96	0.12	12	0.1

With the bioavailability issue addressed, we returned to the more potent of compounds **2–25** in efforts to obtain a better understanding of the in vitro pharmacology of the series. As shown in Table 1, *h*-DDO selectivity was not an issue because all compounds tested had only weak *h*-DDO activity. Rat DAAO enzyme (*r*-DAAO) activity was determined for most of the compounds in Table 1, and *r*-DAAO potencies were found to be 10–500 fold weaker than *h*-DAAO. Specifically, compound **2** was 54× less active at the rat enzyme (IC₅₀ = 215 nM), possibly explaining the high free brain exposure (670 nM) necessary to increase in vivo D-serine levels in the rat. We also found the literature compound, pyrrole carboxylic acid **1**, to be 50× weaker against the rat enzyme. Comparing *h*- and *r*-DAAO enzyme, there is one deletion in *r*-DAAO that is near the VAAGL hydrophobic stretch (L27 in human), and we speculate that this may change the conformation of *r*-DAAO around that area.³⁴ SAR derived from the *r*-DAAO data suggested that either halogen substitution at the 5-position of the quinolinone ring (**6** and **10**) or replacement of the 8-carbon atom with nitrogen (**18**) alleviated the potency differences between *r*- and *h*-DAAO. In efforts to confirm *h*-DAAO binding affinity (*K*_D), the most potent compounds from Table 1 were evaluated in a Biacore assay and the data is presented in Table 3. The *K*_D for most compounds tested was 2–4 fold weaker than the *h*-DAAO IC₅₀ data, with the exception of 1,8-naphthyridinone **18**, which had a *K*_D of 2 nM (4× more potent than its IC₅₀). We were excited to find that the potent binding affinity of **18** was due in part to a slower off rate (*k*_{off} = 6 × 10⁻⁴).

Compound **26** was designed by combining the 6-fluoro substitution (**5**) that provided enhanced oral bioavailability with the 4-chloro group (**10**) that allowed for improved activity at the rat receptor. Incorporating further the 1,8-naphthyridinone ring of **18** that improved *h*-DAAO binding affinity (Biacore assay) led to **27**, the first compound in this series with single digit nM activity against both the *r*- and *h*-DAAO enzyme (see Table 1).

In efforts to improve in vivo screening throughput and reduce the amount of compound required for testing, we chose to use the mouse (instead of the rat) to evaluate a compound's ability to increase cerebellum D-serine levels. Screening at 10 mg/kg, sc in the mouse, Figure 4 shows the magnitude of cerebellum D-serine changes for compounds **1**, **2**, **4**, **5**, **7**, **14**, **15**, and **27**. Compound **27**, the only analogue of **2** that increased D-serine at this dose, is also the only compound tested with *r*-DAAO IC₅₀ < 10 nM. Free brain exposures of compounds **1**, **2**, and **27** in this experiment (Table 4) revealed that **1** and **27** had exposures 2.6- and 3-fold over their *r*-DAAO IC₅₀'s, whereas compound **2** had a free brain exposure 14-fold below its *r*-DAAO IC₅₀ of 215 nM. This data suggests that a compound with free brain concentrations greater than its IC₅₀ in the *r*-DAAO assay should increase cerebellum D-serine levels in the mouse.

Conclusions

The 3-hydroxyquinolin-2(1H)-one **2** is a potent *h*-DAAO inhibitor that binds within the small active site in a similar manner as benzoic acid binds to *h*-DAAO. Placement of small groups around the quinolinone ring and/or replacement of ring

carbon atoms with nitrogen did not further improve the *h*-DAAO potency of **2**. However, fluoro substitution at the 6- or 7-position improved oral bioavailability, chloro substitution at the 5-position improved *r*-DAAO potency, and replacement of the 8-carbon atom with nitrogen improved *h*-DAAO binding affinity. The accumulation of these three SAR features led to the design of **27**, a 4 nM DAAO inhibitor against both rat and human enzyme that elevated D-serine levels in the mouse at free brain exposures three times its rat IC₅₀. We conclude that the ability of a compound to increase cerebellum D-serine levels can be predicted based on free brain exposure versus its potency in the same (or similar) species. The relationship of cerebellum D-serine levels to activity in animal models will be reported in future publications.

Experimental Section

Biology. DAAO in Vitro Activity Assay. Inhibitor compounds are diluted in 100% DMSO starting at 4 mM in half log increments to create an 11-point dose response curve. Each dilution is spotted in duplicate, 0.5 μL/well, into black 384-well plates (Costar no. 3573). No inhibition control wells (ZPE) were spotted with 0.5 μL of 100% DMSO, and 100% inhibition control wells (HPE) were spotted with 0.5 μL of 4 mM 3-hydroxyquinolin-2(1H)-one in 100% DMSO. Then 20 μL of assay buffer (100 mM Tris-HCL, pH 8.5) containing 4 nM human or 40 nM rat DAAO enzyme expressed in sf9 insect cells (produced and purified in-house), 80 μM flavin adenine dinucleotide (Sigma no. F6625), 0.8 units horseradish peroxidase (Sigma no. P8250), and 100 μM Amplex Red (Molecular Probes no. A12222) were added to each well of the plate using a Titertek MultiDrop-384 reagent addition device. Next, 20 microliters of assay buffer containing D-serine (Sigma no. S4250) 0.4 mM for human or 20 mM for rat DAAO were added using the MultiDrop. The plates were spun at 1000 rpm to ensure all liquid was coalesced to the bottom of the well. Exposure of Amplex Red to light must be kept to a minimum. The reaction was then incubated in the dark at ambient temperature for 10–30 min before reading the plates on a Perkin-Elmer Envision 2103 multilabel reader using the following settings: 10 flashes of the flash lamp, excitation filter 530 nm, emission filter 590 nm. The mean of the plate HPE and ZPE control values was used to calculate % inhibition values for each compound well, and nonlinear curve fitting was used to calculate an IC₅₀ value for each compound.

DDO in Vitro Activity Assay. The assay to measure DDO activity was identical to the DAAO assay with the following exceptions. Human DDO enzyme 0.2 nM, also expressed and purified from sf9 insect cells in-house, was substituted for DAAO and D-serine was replaced with 0.5 mM D-aspartic acid (Sigma no. 219096). The 100% inhibition control wells (HPE) were spotted with 0.5 μL of 4 mM 1-naphthol in 100% DMSO.

Biacore Binding of DAAO Inhibitors. A custom Neutravidin surface was generated using standard amine coupling methods from Biacore on a CM5 sensor chip. An enzymatically biotinylated *h*-DAAO was immobilized onto the Neutravidin surface to a level of ~9000 Ru. Binding studies were performed in 100 mM TRIS, 150 mM NaCl, 0.05% P20, 50 μM FAD, 3% DMSO, pH 8.5 at 25 °C in a Biacore 3000 (GE Healthcare) instrument. Compounds were injected at three concentrations, and binding responses were processed using Scrubber 2 (BioLogic Software, Inc.) to align and double reference the data. The kinetic data were fit globally to a simple 1:1 interaction model using Biaeval (GE Healthcare) to obtain the rate constants and affinity.

In Vivo Activity of DAAO Inhibitors. Male Sprague–Dawley CD rats (Charles River Laboratories) or male 129/SVEV mice (Taconic Laboratories, Hudson, NY) were housed under a 12 h light–dark cycle with lights on at 0600. Food and water was provided ad libitum, and animals were acclimated for 5–7 days. Animals were handled and cared for according to the Guide for the Care and Use of Laboratory Animals (National Research Council, 1996), and all procedures were performed with the approval of the Pfizer Animal Care and Use Committee. Rats were dosed sc at 1–2 mL/kg and mice at 10 mL/kg with vehicle alone or compound prepared in 5/5/90 vehicle (5% DMSO, 5% Cremophor EL (Fluka), 90% 0.9% sodium chloride solution). At 4 h post injection, animals were anesthetized using CO₂ gas and cerebella were dissected out and stored at –80 °C until processed for D-serine measurements. Tissue was homogenized in 3 volumes PBS with a 5 mm stainless steel bead in a MixerMill 300 (Qiagen). Homogenate was mixed with 16 volumes of HPLC grade acetonitrile and centrifuged at 13000 rpm in refrigerated microcentrifuge for 15 min. A 0.1–0.2 mL aliquot of the supernatant was dried down in a speed vacuum system and stored at –20 °C prior to analysis.

D-Serine Assay. Calibration Standards. Stock solutions of D-serine (2 mg/mL, Fluka no. 84970) and ¹³C₃, ¹⁵N DL-serine (internal standard, 2 mg/mL, Cambridge Isotope Laboratories, no. CNLM-4207) were prepared individually in HPLC-grade water. Calibration standard (CS) samples were prepared by serial dilution of D-serine stock solution with methanol/water (80/20) to yield concentrations of 0.003, 0.006, 0.012, 0.023, 0.047, 0.094, 0.188, 0.375, 0.750, 1.50, and 3.00 µg/mL. Quality control (QC) samples were similarly prepared to concentrations of 0.01, 0.1, and 1.0 µg/mL. CS and QC samples were extracted with 4 volumes of acetonitrile, centrifuged, and the supernatants evaporated to dryness under a stream of nitrogen. Sets of dried CS and QC samples were stored at –20 °C until needed.

Sample Preparation. Aliquots of tissue samples, CS and QC aliquots (previously extracted and dried), were reconstituted in LC/MS buffer [95:5 methanol/(water + 10 mM ammonium formate + 0.1% formic acid)]. Internal standard DL-serine had been previously added to the LC/MS buffer to a concentration of 0.5 µg/mL. Dried samples were reconstituted to original volume, sonicated for 3 min, and vortexed for 1 min.

LC/MS-MS Conditions. A Shimadzu LC-10AD equipped with a degasser and a CTC Analytics HTS PAL autosampler (Leap Technologies) were used to inject 10 µL aliquots of the processed samples/calibration standards/QC's onto an Astec Chirobiotic-T column (2.1 mm × 250 mm, 5 µm), run isocratically. The mobile phase was a 95/5 mixture of mobile phase A (methanol) and phase B (water + 10 mM ammonium formate + 0.1% formic acid). Quantitation was achieved by MS/MS detection in positive ion mode for analyte and internal standard using a Thermo Quantum Ultra triple quadrupole mass spectrometer equipped with an ESI source. Detection of the ions was performed in the selected reaction monitoring (SRM) mode, monitoring the transition of *m/z* 106.1 → 60.1 for D-serine and *m/z* 110 → 63.1 for the internal standard. The analytical data were processed by Xcalibur software (version 2). Calibration curves were acquired by plotting the peak area ratio of analyte to internal standard against the nominal concentration of calibration standards. Standard curves were calculated with a 4-parameter fit analysis using a 1/*y* weighting factor.

Chemistry. General Methods. Solvents and reagents were of reagent grade and were used as supplied by the manufacturer. All reactions were run under a N₂ atmosphere. Organic extracts were routinely dried over anhydrous Na₂SO₄. Concentration refers to rotatory evaporation under reduced pressure. Chromatography refers to flash chromatography using disposable RediSepR_f 4g silica columns on a CombiFlash Companion automated system. Elemental analyses were performed by QTI, Whitehouse, NJ (compounds **2**, **4**, **5**, and **18**). All target compounds were analyzed using ultra high performance liquid chromatography/UV/ evaporative light scattering detection coupled to time-of-flight mass spectrometry (UHPLC/UV/ELSD/TOFMS). Unless otherwise noted, all tested compounds

were found to be ≥95% pure by this method. Reference compound **1** was prepared using literature procedures.³⁵

UHPLC/MS Analysis. The UHPLC was performed on a Waters ACQUITY UHPLC system (Waters, Milford, MA), which was equipped with a binary solvent delivery manager, column manager, and sample manager coupled to ELSD and UV detectors (Waters, Milford, MA). Detection was performed on a Waters LCT premier XE mass spectrometry (Waters, Milford, MA). The instrument was fitted with an Acquity BEH (bridged ethane hybrid) C18 column (30 mm × 2.1 mm, 1.7 µm particle size, Waters, Milford, MA) operated at 60 °C.

General Procedure A. 7-Fluoro-3-hydroxyquinolin-2(1H)-one (4). **Step 1.** 6-Fluoro-1H-indole-2,3-dione (200 mg, 1.2 mmol), diethylamine (0.24 mL, 2.3 mmol), and ethyl diazoacetate (0.24 mL, 2.3 mmol) were dissolved in ethanol (15 mL) and stirred at room temperature for 64 h. Removal of solvent in vacuo then provided the diazo intermediate as an oil (LCMS *m/z* 278.0 [M-1]); this was treated with 1 N HCl (75 mL) and allowed to react for 40 h at room temperature. Filtration of the reaction mixture yielded ethyl 7-fluoro-3-hydroxy-2-oxo-1,2-dihydroquinoline-4-carboxylate as an orange solid (144 mg, 48% yield). LCMS *m/z* 252.1 (M + 1). ¹H NMR (400 MHz, CD₃OD) δ 1.42 (t, *J* = 7.0 Hz, 3H), 4.48 (q, *J* = 7.0 Hz, 2H), 7.02 (m, 2H), 7.67 (dd, *J* = 5.6, 8.9 Hz, 1H).

Step 2. Methanol (7.5 mL), water (7.5 mL), and the compound from step 1 (100 mg, 0.4 mmol) were combined in a 30 mL microwave tube and treated with LiOH (86 mg, 3.6 mmol). The reaction was subjected to microwave conditions (Biotage Advancer, 150 °C, high power) for 2 h, with 30 s of prestirring. A white solid was removed via filtration, and the filtrate was acidified to pH 0 with 1 N HCl. Filtration of the resulting precipitate provided the title compound as a beige solid (70 mg, 68% yield). MS (APCI) *m/z* 180.0 (M + 1). ¹H NMR (400 MHz, CD₃OD) δ 6.98 (m, 2H), 7.13 (br s, 1H), 7.51 (dd, *J* = 6.0, 8.5 Hz, 1H).

General Procedure B. 3-Hydroxy-1,8-naphthyridin-2(1H)-one Hydrobromide (18). **Step 1.** Ethyl methoxyacetate (0.71 mL, 6.0 mmol) was added to a –78 °C solution of lithium bis(trimethylsilyl)amide (1.0 M solution in THF, 6.0 mL, 6.0 mmol) in THF (6 mL). After 20 min, a solution of 2-aminonicotinaldehyde (244 mg, 2.0 mmol) in THF (4 mL) was added. The resulting orange solution was allowed to come slowly to room temperature as the dry ice/acetone bath warmed up. After 18 h, the reaction was quenched with 6 N HCl (2.2 mL, 13.2 mmol), providing a precipitate; this mixture was heated to reflux for 1 h, then allowed to stir at room temperature for 65 h. The liquid was decanted off, and the semisolids were washed with DCM and triturated with MeOH, providing 3-methoxy-1,8-naphthyridin-2(1H)-one as an off-white solid (167 mg, 48% yield). LCMS *m/z* 175.1 (M – 1). ¹H NMR (400 MHz, DMSO-*d*₆) δ 3.82 (s, 3H), 7.21 (dd, *J* = 7.7, 4.8 Hz, 1H), 7.23 (s, 1H), 8.00 (dd, *J* = 7.8, 1.8 Hz, 1H), 8.35 (dd, *J* = 4.8, 1.9 Hz, 1H), 12.28 (br s, 1H).

Step 2. 3-Methoxy-1,8-naphthyridin-2(1H)-one (20 mg, 0.11 mmol) was mixed with anhydrous DCM (2 mL) and cooled in a dry ice/acetone bath. BBr₃ (1.0 M solution in DCM, 0.46 mL, 0.46 mmol) was added, and the reaction was allowed to slowly warm to room temperature. After stirring for 18 h, the reaction was cooled to –78 °C again and quenched with methanol (5 mL). The mixture was warmed to ambient temperature, solvents were removed under reduced pressure, and the residue was triturated with DCM to provide an off-white solid (23 mg, 86% yield). LCMS *m/z* 161.1 (M – 1). ¹H NMR (400 MHz, CD₃OD) δ 7.30 (s, 1H), 7.58 (dd, *J* = 7.9, 5.8 Hz, 1H), 8.46 (m, 2H). UHPLC: 94%(UV), 100% (ELSD).

3-Hydroxyquinolin-2(1H)-one (2). **General Procedure A, Step 1.** Ethyl 3-hydroxy-2-oxo-1,2-dihydroquinoline-4-carboxylate was prepared from 1H-indole-2,3-dione. Yellow solid (79% yield). LCMS *m/z* 232.2 (M – 1). ¹H NMR (400 MHz, CDCl₃) δ 1.53 (t, *J* = 7.1 Hz, 3H), 4.60 (q, *J* = 7.1 Hz, 2H), 7.30 (m, 1H), 7.37 (d, *J* = 8.3 Hz, 1H), 7.43 (m, 1H), 8.13 (dd, *J* = 8.3, 1.1 Hz, 1H), 10.16 (br s, 1H), 11.28 (br s, 1H).

Step 2. Product was triturated with MeOH and EtOAc. Light-brown solid (17% yield). LCMS *m/z* 160.4 (M – 1). ¹H NMR (400

MHz, DMSO- d_6) δ 7.08 (s, 1H), 7.12 (ddd, $J = 7.9, 6.8, 1.7$ Hz, 1H), 7.27 (m, 2H), 7.49 (d, $J = 7.9$ Hz, 1H), 9.46 (br s, 1H), 12.01 (br s, 1H).

8-Fluoro-3-hydroxyquinolin-2(1H)-one (3). General Procedure A, Step 1. Ethyl 8-fluoro-3-hydroxy-2-oxo-1,2-dihydroquinoline-4-carboxylate was prepared from 7-fluoro-1H-indole-2,3-dione. Orange solid (68% yield). LCMS m/z 250.1 ($M - 1$). ^1H NMR (400 MHz, CD_3OD) δ 1.42 (t, $J = 7.1$ Hz, 3H), 4.49 (q, $J = 7.1$ Hz, 2H), 7.19 (m, 2H), 7.41 (m, 1H).

Step 2. Product was rinsed with pH 7 buffer, then methanol. Tan solid (55% yield). LCMS m/z 178.0 ($M - 1$). ^1H NMR (400 MHz, DMSO- d_6) δ 7.10 (ddd, $J = 8, 8, 5.2$ Hz, 1H), 7.13 (d, $J = 1.6$ Hz, 1H), 7.18 (ddd, $J = 10.3, 8.1, 1.4$ Hz, 1H), 7.32 (br d, $J = 7.8$ Hz, 1H), 9.74 (br s, 1H), 12.06 (br s, 1H).

6-Fluoro-3-hydroxyquinolin-2(1H)-one (5). General Procedure A, Step 1. Ethyl 6-fluoro-3-hydroxy-2-oxo-1,2-dihydroquinoline-4-carboxylate was prepared from 5-fluoro-1H-indole-2,3-dione. Gray solid (85% yield). LCMS m/z 250.2 ($M - 1$).

Step 2. Product was triturated with a mixture of MeOH/EtOAc. Brown solid (19% yield). LCMS m/z 178.1 ($M - 1$). ^1H NMR (400 MHz, DMSO- d_6) δ 7.06 (s, 1H), 7.14 (ddd, $J = 8.7, 8.7, 2.9$ Hz, 1H), 7.24 (dd, $J = 8.9, 5.2$ Hz, 1H), 7.33 (dd, $J = 9.5, 2.9$ Hz, 1H), 9.70 (br s, 1H), 12.06 (br s, 1H).

5-Fluoro-3-hydroxyquinolin-2(1H)-one (6). Step 1. Ethyl methoxyacetate (253 μL , 2.15 mmol) was added to a solution of lithium bis(trimethylsilyl)amide (1.0 M solution in tetrahydrofuran, 2.2 mL, 2.2 mmol) in THF (2 mL) at -78°C . After 20 min, a solution of 2-amino-6-fluorobenzaldehyde (100 mg, 0.719 mmol) in THF (2 mL) was added dropwise. The resulting yellow solution was kept at -78°C for 15 min and then allowed to warm to room temperature, then 6 N HCl (360 μL , 2.2 mmol) was added and the precipitate was collected by filtration. Purification by chromatography (gradient: 100% DCM to 5:1 DCM:MeOH) provided 5-fluoro-4-hydroxy-3-methoxy-3,4-dihydroquinolin-2(1H)-one. White solid (100 mg, 65% yield). MS (APCI) m/z 209.8 ($M - 1$). ^1H NMR (400 MHz, CD_3OD) δ 3.64 (s, 3H), 4.11 (d, $J = 3.7$ Hz, 1H), 5.24 (d, $J = 3.7$ Hz, 1H), 6.73 (d, $J = 8.0$ Hz, 1H), 6.80 (br dd, apparent t, $J = 9, 9$ Hz, 1H), 7.29 (ddd, apparent td, $J = 8.2, 8.2, 6.0$ Hz, 1H). Partial ^1H NMR of minor diastereomer: δ 3.45 (s, 3H), 3.77 (d, $J = 3.1$ Hz, 1H), 5.02 (d, $J = 2.9$ Hz, 1H).

General Procedure B, Step 2. Tan solid, 91% yield. LCMS m/z 180.1 ($M + 1$). ^1H NMR (400 MHz, CD_3OD) δ 6.95 (dd, $J = 10.1, 8.0$ Hz, 1H), 7.12 (d, $J = 8.4$ Hz, 1H), 7.27 (s, 1H), 7.32 (ddd, apparent td, $J = 8.2, 8.2, 5.8$ Hz, 1H). UHPLC: 93% (UV), 100% (ELSD).

8-Chloro-3-hydroxyquinolin-2(1H)-one (7). General Procedure A, Step 1. Ethyl 8-chloro-3-hydroxy-2-oxo-1,2-dihydroquinoline-4-carboxylate was prepared from 7-chloro-1H-indole-2,3-dione. Yellow solid (78% yield). LCMS m/z 266.1 ($M - 1$).

Step 2. Product was triturated with EtOAc. Yellow solid (11% yield). LCMS m/z 194.2 ($M - 1$). ^1H NMR (400 MHz, DMSO- d_6) δ 7.14 (dd, $J = 7.8, 7.8$ Hz, 1H), 7.15 (s, 1H), 7.43 (dd, $J = 7.8, 1.3$ Hz, 1H), 7.50 (dd, $J = 8.0, 1.2$ Hz, 1H), 9.86 (br s, 1H), 11.37 (br s, 1H).

7-Chloro-3-hydroxyquinolin-2(1H)-one (8). General Procedure A. Purified by precipitating out of hot methanol. White amorphous solid (51% yield). LCMS m/z 194.0 ($M - 1$). ^1H NMR (400 MHz, DMSO- d_6) δ 6.59 (s, 1H), 7.03 (dd, $J = 8.5, 2.1$ Hz, 1H), 7.20 (d, $J = 2.1$ Hz, 1H), 7.29 (d, $J = 8.5$ Hz, 1H).

6-Chloro-3-hydroxyquinolin-2(1H)-one (9). General Procedure A, Step 1. Ethyl 6-chloro-3-hydroxy-2-oxo-1,2-dihydroquinoline-4-carboxylate was prepared from 5-chloro-1H-indole-2,3-dione. Gray solid (66% yield). LCMS m/z 266.1 ($M - 1$).

Step 2. Beige solid (66% yield). LCMS m/z 196.1 ($M + 1$). ^1H NMR (400 MHz, DMSO- d_6) δ 7.07 (s, 1H), 7.24 (d, $J = 8.7$ Hz, 1H), 7.31 (dd, $J = 8.7, 2.5$ Hz, 1H), 7.61 (d, $J = 2.5$ Hz, 1H), 9.77 (br s, 1H), 12.13 (br s, 1H).

General Procedure C. 5-Chloro-3-hydroxyquinolin-2(1H)-one (10). Step 1. 4-Chloro-1H-indole-2,3-dione (182 mg, 1.00 mmol), diethylamine (0.207 mL, 2.0 mmol), and (trimethylsilyl)diazomethane (2 M solution in hexanes, 1.0 mL, 2.0 mmol) were

dissolved in ethanol (5 mL) and stirred at 25°C . After 18 h, the resulting heterogeneous mixture was filtered and the solid was rinsed with ethanol (2×1 mL) to provide 125 mg of 5-chloro-3-methoxyquinolin-2(1H)-one as a gray solid. LCMS m/z 210.1 ($M + 1$).

Step 2. The title compound was prepared according to general procedure B, step 2, except that 5-chloro-3-methoxyquinolin-2(1H)-one was used as the starting material and the crude product was slurried with hot methanol rather than triturated with DCM. Gray solid (70% yield). LCMS m/z 194.0 ($M - 1$). ^1H NMR (400 MHz, DMSO- d_6) δ 7.22 (s, 1H), 7.27 (m, 3H), 10.03 (br s, 1H), 12.24 (br s, 1H).

3-Hydroxy-8-methylquinolin-2(1H)-one (11). General Procedure A, Step 1. Ethyl 3-hydroxy-8-methyl-2-oxo-1,2-dihydroquinoline-4-carboxylate was prepared from 7-methyl-1H-indole-2,3-dione. Beige solid (38% yield). LCMS m/z 246.2 ($M - 1$). ^1H NMR (400 MHz, CDCl_3) δ 1.50 (t, $J = 7.0$ Hz, 3H), 2.49 (s, 3H), 4.57 (q, $J = 7.0$ Hz, 2H), 7.20 (dd, $J = 8, 7.5$ Hz, 1H), 7.27 (obscured by solvent peak, presumed 1H), 7.85 (d, $J = 7.5$ Hz, 1H), 9.29 (br s, 2H).

Step 2. Purified by two sequential preparative thin layer chromatographic separations on silica gel (1:1 ethyl acetate: hexanes). Gray solid (23% yield). LCMS m/z 174.2 ($M - 1$). ^1H NMR (400 MHz, CDCl_3) δ 2.50 (s, 3H), 6.83 (br s, 1H), 7.16 (dd, $J = 7.5, 7.5$ Hz, 1H), 7.20 (s, 1H), 7.24 (br d, $J = 7.5$ Hz, 1H), 7.39 (br d, $J = 7.5$ Hz, 1H), 9.51 (br s, 1H).

3-Hydroxy-7-methylquinolin-2(1H)-one (12). General Procedure A. Tan solid (88% yield). LCMS m/z 174.1 ($M - 1$). ^1H NMR (400 MHz, DMSO- d_6) δ 2.32 (s, 3H), 6.94 (d, $J = 8.0$ Hz, 1H), 6.98 (s, 1H), 7.04 (s, 1H), 7.34 (d, $J = 8.0$ Hz, 1H).

3-Hydroxy-6-methylquinolin-2(1H)-one (13). General Procedure A, Step 1. Ethyl 3-hydroxy-6-methyl-2-oxo-1,2-dihydroquinoline-4-carboxylate was prepared from 5-methyl-1H-indole-2,3-dione. Purification by chromatography (gradient: 3% ethyl acetate/heptane to 100% ethyl acetate); dark-yellow solid (36% yield). LCMS m/z 248.1 ($M + 1$). ^1H NMR (400 MHz, CDCl_3) δ 1.52 (t, $J = 7.0$ Hz, 3H), 2.44 (s, 3H), 4.59 (q, $J = 7.0$ Hz, 2H), 7.26 (m, 2H), 7.84 (s, 1H), 9.72 (br s, 1H), 11.47 (br s, 1H).

Step 2. Purified by preparative silica gel thin layer chromatography (70% ethyl acetate/hexanes); grayish-beige solid (25% yield). LCMS m/z 174.2 ($M - 1$). ^1H NMR (400 MHz, CDCl_3) δ 2.42 (s, 3H), 6.85 (br s, 1H), 7.14 (s, 1H), 7.15 (m, 1H), 7.21 (m, 1H), 7.30 (s, 1H), 10.33 (br s, 1H).

3-Hydroxy-5-methylquinolin-2(1H)-one (14). General Procedure B, Step 1. 3-Methoxy-5-methylquinolin-2(1H)-one was prepared from 2-amino-6-methylbenzaldehyde. Purification by chromatography (gradient: DCM to 5:1 DCM:MeOH). The product crystallized out of one of the fractions and was collected by filtration. White crystalline solid (17% yield). MS (APCI) m/z 187.8 ($M - 1$). ^1H NMR (400 MHz, CD_3OD) δ 2.56 (s, 3H), 3.95 (s, 3H), 7.09 (d, $J = 7.2$ Hz, 1H), 7.16 (d, $J = 8.2$ Hz, 1H), 7.27 (m, 1H), 7.29 (s, 1H).

Step 2. Tan solid, quantitative yield. LCMS m/z 176.1 ($M + 1$). ^1H NMR (400 MHz, CD_3OD) δ 2.55 (s, 3H), 7.20 (d, $J = 7.0$ Hz, 1H), 7.30 (d, $J = 7.8$ Hz, 1H), 7.36 (dd, $J = 7.2, 7.2$ Hz, 1H), 7.57 (s, 1H).

5-Ethyl-3-hydroxyquinolin-2(1H)-one (15). General Procedure C, Step 1. A mixture of 5-ethyl-3-methoxyquinolin-2(1H)-one and 5-ethyl-3-hydroxyquinolin-2(1H)-one was prepared from 4-ethylindoline-2,3-dione. Tan solid (59% yield). Without further purification, the mixture was carried directly to next step.

Step 2. Brown solid (91% yield). LCMS m/z 190.1 ($M + 1$). ^1H NMR (400 MHz, CD_3OD) δ 1.30 (tr, $J = 7.6$ Hz, 3H), 2.94 (q, $J = 7.6$ Hz, 2H), 7.18 (d, $J = 8.0$ Hz, 1H), 7.27 (d, $J = 8.2$ Hz, 1H), 7.37 (m, 1H), 7.55 (s, 1H).

7-Ethyl-3-hydroxyquinolin-2(1H)-one (16). General Procedure A, Step 1. Ethyl 7-ethyl-3-hydroxy-2-oxo-1,2-dihydroquinoline-4-carboxylate was prepared from 6-ethyl-1H-indole-2,3-dione. Purified by chromatography (gradient: 50% EtOAc/heptane to 100% EtOAc), 45% yield, LCMS m/z 260.2 ($M - 1$), containing ~5% 6-ethyl-1H-indole-2,3-dione.

Step 2. Purified by column chromatography (gradient: 5% EtOAc/heptane to 100% EtOAc), followed by preparative silica gel TLC (50% EtOAc/hexanes). Brown solid (1.9 mg, 0.01 mmol, 5% yield). LCMS m/z 188.2 ($M - 1$). $^1\text{H NMR}$ (400 MHz, CDCl_3) δ 1.28 (t, 3H, presumed—obscured by solvent), 2.74 (q, $J = 7.5$ Hz, 2H), 6.87 (s, 1H), 7.11 (m, 2H), 7.20 (s, 1H), 7.43 (d, $J = 8.1$ Hz, 1H), 11.15 (br s, 1H).

8-Ethyl-3-hydroxyquinolin-2(1H)-one (17). General Procedure C, Step 1. Purified by TLC prep plate (1:1 EtOAc/heptane and 1% triethylamine). White gummy solid (10% yield). LCMS m/z 190.1 ($M + 1$). $^1\text{H NMR}$ (400 MHz, CD_3OD) δ 1.30 (tr, $J = 7.5$ Hz, 3H), 2.90 (q, $J = 7.5$ Hz, 2H), 7.15 (m, 2H), 7.24 (d, $J = 7.3$ Hz, 1H), 7.35 (d, $J = 7.7$ Hz, 1H).

3-Hydroxy-1,6-naphthyridin-2(1H)-one Hydrobromide (19). General Procedure B, Step 1. 3-Methoxy-1,6-naphthyridin-2(1H)-one was prepared from 4-aminonicotinaldehyde. The residue was triturated with ether to provide a tan solid which was subsequently subjected to DCVC³⁶ over silica gel (gradient: 100% DCM to 10:1 DCM:MeOH). White solid, 56% yield. APCI m/z 175.1 ($M - 1$). $^1\text{H NMR}$ (400 MHz, CD_3OD) δ 3.96 (s, 3H), 7.37 (s, 1H), 7.39 (m, apparent br d, $J = 6.0$ Hz, 1H), 8.40 (d, $J = 6.0$ Hz, 1H), 8.86 (s, 1H).

Step 2. A mixture of 3-methoxy-1,6-naphthyridin-2(1H)-one (25 mg, 0.14 mmol) in anhydrous DCM (2 mL) at -78°C was treated with BBr_3 (1.0 M solution in dichloromethane, 1.14 mL, 1.14 mmol). After 4 d at ambient temp, the mixture was cooled to -78°C and quenched with methanol (5 mL). The resulting mixture was warmed to room temp, concentrated, and the residue was triturated sequentially with DCM, EtOAc, and hot MeOH. Off-white solid (13.2 mg, 0.054 mmol, 39% yield). APCI m/z 161.1 ($M - 1$). $^1\text{H NMR}$ (400 MHz, CD_3OD) δ 7.27 (s, 1H), 7.62 (d, $J = 6.6$ Hz, 1H), 8.46 (m, apparent br d, $J = 6.6$ Hz, 1H), 8.98 (s, 1H).

3-Hydroxy-1,7-naphthyridin-2(1H)-one Hydrobromide (20). General Procedure B, Step 1. 3-Methoxy-1,7-naphthyridin-2(1H)-one was prepared from 3-aminoisonicotinaldehyde. Light-yellow solid, 25% yield. LCMS m/z 175.1 ($M - 1$). $^1\text{H NMR}$ (400 MHz, CD_3OD) δ 3.97 (s, 3H), 7.25 (s, 1H), 7.60 (d, $J = 5.4$ Hz, 1H), 8.27 (d, $J = 5.4$ Hz, 1H), 8.54 (s, 1H).

Step 2. To a stirred mixture of methoxy-1,7-naphthyridin-2(1H)-one (10.9 mg, 0.062 mmol) in anhydrous DCM (2 mL) at -78°C was added BBr_3 (1.0 M solution in DCM, 1.32 mL, 1.32 mmol). After stirring for 7 days at ambient temp, the mixture was cooled to 0°C and quenched with methanol (4 mL). The mixture was warmed to room temperature, solvents were removed under reduced pressure, and the residue was triturated with DCM and then with 20:1 DCM:MeOH. Light-gray solid (8 mg, 0.033 mmol, 53% yield). LCMS m/z 161.1 ($M - 1$). $^1\text{H NMR}$ (400 MHz, CD_3OD) δ 7.28 (s, 1H), 8.02 (d, $J = 6.2$ Hz, 1H), 8.36 (d, $J = 6.2$ Hz, 1H), 8.61 (s, 1H).

3-Hydroxy-1,5-naphthyridin-2(1H)-one Hydrobromide (21). General Procedure B, Step 1. 3-Methoxy-1,5-naphthyridin-2(1H)-one was prepared from 3-aminopyridine-2-carbaldehyde. White solid, 55% yield. LCMS m/z 175.1 ($M - 1$). $^1\text{H NMR}$ (400 MHz, CD_3OD) δ 3.98 (s, 3H), 7.26 (s, 1H), 7.41 (dd, $J = 4.6, 8.3$ Hz, 1H), 7.70 (br d, $J = 8.3$ Hz, 1H), 8.45 (dd, $J = 1.2, 4.6$ Hz, 1H).

Step 2. In a microwave vial equipped with a stir bar, finely ground product from step 1 (10 mg, 0.06 mmol) was mixed with anhydrous DCM (1 mL) and cooled in a dry ice/acetone bath. BBr_3 (1.0 M solution in DCM, 0.38 mL, 0.38 mmol) was added and the reaction was warmed to room temperature over 20 min and then heated in a microwave reactor for 10 min at 100°C . The tightly capped reaction was then subjected to conventional heating at 60°C . After 65 h, the mixture was cooled to 0°C , MeOH (3 mL) was added, and the resulting mixture was concentrated in vacuo and the residue was triturated with DCM and filtered. Gray solid (10.8 mg, 0.044 mmol, 73%). LCMS m/z 161.0 ($M - 1$). $^1\text{H NMR}$ (400 MHz, CD_3OD) δ 7.23 (s, 1H), 7.79 (dd, $J = 5.7, 8.4$ Hz, 1H), 8.20 (d, $J = 8.0$ Hz, 1H), 8.53 (dd, $J = 1.2, 5.7$ Hz, 1H).

7-Hydroxypyrido[2,3-*b*]pyrazin-6(5H)-one (22). General Procedure B, Step 1. Solid was dissolved in MeOH and filtered through a $0.2\ \mu\text{m}$ nylon membrane 13 mm syringe filter. Filtrate was concentrated to give an amorphous solid. LCMS m/z 164.1 ($M + 1$). $^1\text{H NMR}$ (400 MHz, CD_3OD) δ 6.13 (s, 1H), 8.52 (d, $J = 2.2$ Hz, 1H), 8.61 (d, $J = 2.0$ Hz, 1H).

3-Hydroxy-4-methylquinolin-2(1H)-one (23). General Procedure B, Step 1. 3-Methoxy-4-methylquinolin-2(1H)-one was prepared from 1-(2-aminophenyl)ethanone. Pink solid (79%). LCMS m/z 190.1 ($M + 1$). $^1\text{H NMR}$ (400 MHz, CD_3OD) δ 2.50 (s, 3H), 3.88 (s, 3H), 7.33 (ddd, $J = 8.2, 7.2, 1.2$ Hz, 1H), 7.37 (br d, $J = 8.3$ Hz, 1H), 7.51 (ddd, $J = 8.3, 7.2, 1.4$ Hz, 1H), 7.80 (br d, $J = 8.2$ Hz, 1H).

Step 2. The residue was triturated with diethyl ether. Pinkish—white solid (8% yield). LCMS m/z 174.1 ($M - 1$). $^1\text{H NMR}$ (400 MHz, CD_3OD) δ 2.40 (s, 3H), 7.26 (ddd, $J = 8.0, 7.0, 1.4$ Hz, 1H), 7.30 (dd, $J = 8.2, 1.3$ Hz, 1H), 7.37 (ddd, $J = 8.2, 7.0, 1.3$ Hz, 1H), 7.68 (dd, $J = 8.0, 0.9$ Hz, 1H).

5-Chloro-6-fluoro-3-hydroxyquinolin-2(1H)-one (26). General Procedure A, Step 1. Ethyl 5-chloro-6-fluoro-3-hydroxy-2-oxo-1,2-dihydroquinoline-4-carboxylate was prepared from 4-chloro-5-fluoro-1H-indole-2,3-dione, except that the aqueous filtrate after HCl treatment was extracted with DCM (2×15 mL) and the combined organic layers concentrated in vacuo to provide additional aliquots of intermediate (total: 220 mg, 0.77 mmol, 77% yield). LCMS m/z 284.1 ($M - 1$).

Step 2. Microwave reaction was carried out for 5 h. Beige solid (9 mg, 0.042 mmol, 9% yield). LCMS m/z 212.1 ($M - 1$). $^1\text{H NMR}$ (400 MHz, $\text{DMSO}-d_6$) δ 7.19 (s, 1H), 7.24 (dd, $J = 4.6, 9.1$ Hz, 1H), 7.35 (dd, $J = 9.1, 9.1$ Hz, 1H), 10.27 (br s, 1H), 12.27 (br s, 1H).

5-Chloro-6-fluoro-3-hydroxy-1,8-naphthyridin-2(1H)-one Hydrobromide (27). General Procedure C, Step 1. 5-Chloro-6-fluoro-3-methoxy-1,8-naphthyridin-2(1H)-one was prepared from 4-Chloro-5-fluoro-1H-pyrrolo[2,3-*b*]pyridine-2,3-dione (30). Beige solid (31 mg, 24% yield). MS m/z 299.1 ($M + 1$). $^1\text{H NMR}$ (400 MHz, $\text{DMSO}-d_6$) δ 3.29 (br s, 3H), 7.12 (br s, 1H), 8.52 (br s, 1H).

Step 2. Beige solid (16 mg, 40% yield). MS m/z 215.1 ($M + 1$). $^1\text{H NMR}$ (400 MHz, $\text{DMSO}-d_6$) δ 7.13 (s, 1H), 8.47 (m, 1H), 12.74 (br s, 1H). UHPLC: 92% (UV), 100% (ELSD).

3,3-Dibromo-4-chloro-5-fluoro-2,3-dihydro-1H-pyrrolo[2,3-*b*]pyridine (29). To a stirred solution of 4-chloro-5-fluoro-1H-pyrrolo[2,3-*b*]pyridine (28) (2 g, 12 mmol) in *tert*-butanol (100 mL) was added *N*-bromosuccinimide (8.35 g, 46.9 mmol). After 2 h, the mixture was concentrated and the residue was dissolved in DCM (100 mL), washed with water (100 mL), and concentrated to give a brownish—beige solid (3.8 g, 94% yield). MS m/z 344.8 ($M + 1$). $^1\text{H NMR}$ (400 MHz, $\text{DMSO}-d_6$) δ 8.45 (d, $J = 2.2$ Hz, 1H), 12.33 (br s, 1H).

4-Chloro-5-fluoro-1H-pyrrolo[2,3-*b*]pyridine-2,3-dione (30). To a stirred solution of 3,3-dibromo-4-chloro-5-fluoro-2,3-dihydro-1H-pyrrolo[2,3-*b*]pyridine (29) (3.8 g, 11 mmol) in 5% H_2O —acetonitrile (150 mL) in an aluminum foil wrapped flask was added silver trifluoroacetate (4.87 g, 22.1 mmol). After stirring at reflux for 1 h, the mixture was cooled to room temp and the precipitated silver bromide was removed by filtration. The dark-green filtrate was concentrated and the residue was triturated with ether and DCM. The combined ether and DCM filtrates were concentrated and purified by chromatography eluting with a gradient of 100% *n*-heptane to 100% ethyl acetate to give a brown solid (114 mg, 5% yield). MS m/z 199.1 ($M - 1$). $^1\text{H NMR}$ (400 MHz, $\text{DMSO}-d_6$) δ 8.54 (d, $J = 2.4$ Hz, 1H), 11.85 (br s, 1H).

Acknowledgment. We thank Brian Rago for analytical support measuring in vivo drug exposures, Katherine Fisher and Jessica Adams for in vitro assay development, Nancy Stratman for [3H]-glycine binding data, and James Valentine and Don Tunucci for high-throughput screening of our compound file.

References

- Wolosker, H. NMDA Receptor Regulation by D-Serine: New Findings and Perspectives. *Mol. Neurobiol.* **2007**, *36*, 152–164.
- Javitt, D. C.; Zukin, S. R. Recent advances in the phencyclidine model of schizophrenia. *Am. J. Psychiatry* **1991**, *148*, 1301–1308.
- Millan, M. J. *N*-Methyl-D-aspartate receptors as a target for improved antipsychotic agents: novel insights and clinical perspectives. *Psychopharmacology* **2005**, *179*, 30–53.
- Hashimoto, K.; Fukushima, T.; Shimizu, E.; Komatsu, N.; Watanabe, H.; Shinoda, N.; Nakazato, M.; Kumakiri, C.; Okada, S.; Hasegawa, H.; Imai, K.; Iyo, M. Decreased serum levels of D-serine in patients with schizophrenia: evidence in support of the *N*-methyl-D-aspartate receptor hypofunction hypothesis of schizophrenia. *Arch. Gen. Psychiatry* **2003**, *60*, 572–576.
- Bendikov, I.; Nadri, C.; Amar, S.; Panizzutti, R.; De Miranda, J.; Wolosker, H.; Agam, G. A CSF and postmortem brain study of D-serine metabolic parameters in schizophrenia. *Schizophrenia Res.* **2007**, *90*, 41–51.
- Madeira, C.; Freitas, M. E.; Vargas-Lopes, C.; Wolosker, H.; Panizzutti, R. Increased brain D-amino acid oxidase (DAAO) activity in schizophrenia. *Schizophrenia Res.* **2008**, *101*, 76–83.
- Burnet, P. W. J.; Eastwood, S. L.; Bristow, G. C.; Godlewska, B. R.; Sikka, P.; Walker, M.; Harrison, P. J. D-Amino acid oxidase activity and expression are increased in schizophrenia. *Mol. Psychiatry* **2008**, *13*, 658–660.
- Verrall, L.; Walker, M.; Rawlings, N.; Benzel, I.; Kew, J. N. C.; Harrison, P. J.; Burnet, P. W. J. D-Amino acid oxidase and serine racemase in human brain: normal distribution and altered expression in schizophrenia. *Eur. J. Neuroscience* **2007**, *26*, 1657–1669.
- Heresco-Levy, U.; Javitt, D. C.; Ebstein, R.; Vass, A.; Lichtenberg, P.; Bar, G.; Catinari, S.; Emilov, M. D-Serine efficacy as add-on pharmacotherapy to risperidone and olanzapine for treatment-refractory schizophrenia. *Biol. Psychiatry* **2005**, *57*, 577–585.
- Tsai, G.; Yang, P.; Chung, L.-C.; Lange, N.; Coyle, J. T. D-Serine added to antipsychotics for the treatment of schizophrenia. *Biol. Psychiatry* **1998**, *44*, 1081–1089.
- Tsai, G. E.; Yang, P.; Chung, L. C.; Tsai, I. C.; Tsai, C. W.; Coyle, J. T. D-Serine added to clozapine for the treatment of schizophrenia. *Am. J. Psychiatry* **1999**, *156*, 1822–5.
- Ferraris, D.; Duvall, B.; Ko, Y.-S.; Thomas, A. G.; Rojas, C.; Majer, P.; Hashimoto, K.; Tsukamoto, T. Synthesis and Biological Evaluation of D-Amino Acid Oxidase Inhibitors. *J. Med. Chem.* **2008**, *51*, 3357–3359.
- Vanoni, M. A.; Cosma, A.; Mazzeo, D.; Mattevi, A.; Todone, F.; Curti, B. Limited Proteolysis and X-ray Crystallography Reveal the Origin of Substrate Specificity and of the Rate-Limiting Product Release during Oxidation of D-Amino Acids Catalyzed by Mammalian D-Amino Acid Oxidase. *Biochemistry* **1997**, *36*, 5624–5632.
- Adage, T.; Trillat, A.-C.; Quattropiani, A.; Perrin, D.; Cavarec, L.; Shaw, J.; Guerassimenko, O.; Giachetti, C.; Greco, B.; Chumakov, I.; Halazy, S.; Roach, A.; Zaratini, P. In vitro and in vivo pharmacological profile of AS057278, a selective D-amino acid oxidase inhibitor with potential antipsychotic properties. *Eur. Neuropsychopharmacol.* **2008**, *18*, 200–214.
- Sparey, T.; Abeywickrema, P.; Slmond, S.; Brandon, N.; Byrne, N.; Campbell, A.; Hutson, P. H.; Jacobson, M.; Jones, B.; Munshi, S.; Pascarella, D.; Pike, A.; Prasad, G. S.; Sachs, N.; Sakatis, M.; Sardana, V.; Venkatraman, S.; Young, M. B. The discovery of fused pyrrole carboxylic acids as novel, potent D-amino acid oxidase (DAO) inhibitors. *Bioorg. Med. Chem. Lett.* **2008**, *18*, 3386–3391.
- Larsen, R. D. Product class 4: quinolinones and related systems. *Sci. Synth.* **2005**, *15*, 551–660.
- Johnsen, B. A.; Undheim, K. *N*-Quaternary Compounds. Part LVI. 3-Hydroxyquinoline-2(1H)-thiones and Their *N*-vinylation. *Acta Chem. Scand., Sect. B* **1984**, 109–112.
- Sit, S.-Y.; Ehrgott, F. J.; Gao, J.; Meanwell, N. A. 3-Hydroxy-quinolin-2-ones: Inhibitors of [³H]-Glycine Binding to the Site Associated with the NMDA Receptor. *Bioorg. Med. Chem. Lett.* **1996**, *6*, 499–504.
- Huntress, E. H.; Bornstein, J.; Hearon, W. M. An Extension of the Diels–Reese Reaction. *J. Am. Chem. Soc.* **1956**, *78*, 2225–2228.
- Fray, J. M.; Bull, D. J.; Carr, C. L.; Stobie, A. Structure–Activity Relationships of 3-Hydroxy-2(1H)-quinolinones as *N*-Methyl-D-Aspartate (Glycine Site) Receptor Antagonists. *Med. Chem. Res.* **1996**, *6*, 581–592.
- Mohammed, Y. S.; Gohar, A. E. M. N.; Abdel-Latif, F. F.; Badr, M. Z. A. Synthesis of 4-substituted-3-hydroxy-2-quinolinones and azines. *Pharmazie* **1985**, *40*, 312–314.
- Manley, P. J.; Bilodeau, M. T. A New Synthesis of Naphthyridinones and Quinolinones: Palladium-Catalyzed Amidation of *o*-Carbonyl-Substituted Aryl Halides. *Org. Lett.* **2004**, *6*, 2433–2435.
- Heller, G.; Fuchs, R.; Jacobsohn, P.; Raschig, M.; Schutze, E. New transformations from the indole into the quinoline series. II. *Ber. Dtsch. Chem. Ges.* **1926**, *59B*, 704–710.
- Park, J.-K.; Im, S.-K.; Ju, H.; Jeon, J.-M.; Kim, C.-G.; Kim, D.-U.; Yoo, J.-C.; Cho, S.-S.; Cho, S.-K. Synthesis and Antibacterial Activity of 1,8-Naphthyridine Cephalosporins. *Bull. Korean Chem. Soc.* **2005**, *26*, 371–372.
- Felix, A. M. Cleavage of Protecting Groups with Boron Tribromide. *J. Org. Chem.* **1974**, *39*, 1427–1429.
- Parrick, J.; Yahya, A.; Ijaz, A. S.; Yizun, J. Convenient Preparation of 3,3-Dibromo-1,3-dihydroindol-2-ones and Indole-2,3-diones (Isatins) from Indoles. *J. Chem. Soc., Perkin Trans. 1* **1989**, 2009–2015.
- Weil, Z. M.; Huang, A. S.; Beigneux, A.; Kim, P. M.; Molliver, M. E.; Blackshaw, S.; Young, S. G.; Nelson, R. J.; Snyder, S. H. Behavioural alterations in male mice lacking the gene for D-aspartate oxidase. *Behav. Brain Res.* **2006**, *171*, 295–302.
- Kawazoe, T.; Park, H. K.; Iwana, S.; Tsuge, H.; Fukui, K. Human D-Amino Acid Oxidase: An Update and Review. *Chem. Rec.* **2007**, *7*, 305–315.
- Mattevi, A.; Vanoni, M. A.; Todone, F.; Rizzi, M.; Teplyakov, A.; Coda, A.; Bolognesi, M.; Curti, B. Crystal structure of D-amino acid oxidase: a case of active site mirror-image convergent evolution with flavocytochrome b₂. *Proc. Natl. Acad. Sci. U.S.A.* **1996**, *93*, 7496–7501.
- Gehlhaar, D. K.; Verkhivker, G. M.; Rejto, P. A.; Sherman, C. J.; Fogel, D. B.; Fogel, L. J.; Freer, S. T. Molecular recognition of the inhibitor AG-1343 by HIV-1 protease: conformationally flexible docking by evolutionary programming. *Chem. Biol.* **1995**, *2*, 317–324.
- Marrone, T.; Luty, B.; Rose, P. Discovering high-affinity ligands from the computationally predicted structures and affinities of small molecules bound to a target: a virtual screening approach. *Perspect. Drug Discovery Des.* **2000**, *20*, 209–230.
- Feng, B.; Mills, J. B.; Davidson, R. E.; Mireles, R. J.; Janiszewski, J. S.; Troutman, M. D.; de Morales, S. M. In vitro P-glycoprotein assays to predict the in vivo interactions of P-glycoprotein with drugs in the central nervous system. *Drug Metab. Dispos.* **2008**, *36* (2), 268–275.
- Baron, B. M.; Siegel, B. W.; Harrison, B. L.; Gross, R. S.; Hawes, C.; Towers, P. ³H]MDL 105,519, A High-Affinity Radioligand for the *N*-Methyl-D-aspartate Receptor-Associated Glycine Recognition Site. *J. Pharmacol. Exp. Ther.* **1996**, *279*, 62–68.
- Kawazoe, T.; Tsuge, H.; Pilone, M. S.; Fukui, K. Crystal structure of human D-amino-acid oxidase: context-dependent variability of the backbone conformation of the VAAGL hydrophobic stretch located at the si-face of the flavin ring. *Protein Sci.* **2006**, *15*, 2708–2717.
- Welch, M.; Phillips, R. S. Improved Syntheses of [3,2-*b*] and [2,3-*b*] Fused Selenolo- and Thienopyrroles, and of Furo[3,2-*b*]pyrrole. *Heterocycl. Commun.* **1999**, *5* (4), 305–310.
- Pedersen, D. S.; Rosenbohm, C. Dry Column Vacuum Chromatography. *Synthesis* **2001**, *16*, 2431–2434.

JM900128W